

In-plane intercalate dynamics in alkali-metal graphite intercalation compounds

W. A. Kamitakahara

Ames Laboratory—United States Department of Energy, Iowa State University, Ames, Iowa 50011

H. Zabel

Department of Physics and Materials Research Laboratory, University of Illinois at Urbana-Champaign, Urbana, Illinois 61801

(Received 23 May 1985)

Inelastic-neutron-scattering methods have been used to investigate the vibrational spectra of the alkali-metal atoms in MC_x compounds, where $M = K, Rb, \text{ or } Cs$, and $x = 8, 24, \text{ or } 36$. Partial phonon densities of states have been determined, in which only in-basal-plane modes associated with the M atoms are represented. The physical origin of M - M forces is discussed. In-plane Debye-Waller factors for the intercalate atoms have been calculated from the observed spectra. For the stage-2 compounds KC_{24} and RbC_{24} , and for the stage-1 compound RbC_8 , detailed measurements of the temperature dependence have been carried out, in order to study the influence of the order-disorder phase transformations which occur, respectively, at 123, 162, and 745 K. Only relatively subtle effects of the phase changes were observed, and the time scale of diffusion in the disordered phases is much longer than that of vibrations, unlike the case of real three-dimensional liquid metals.

I. INTRODUCTION

When graphite is intercalated with an atomic or molecular species (the intercalate), one naturally expects new lattice-vibrational modes to appear which are associated with the intercalate. These can be of two types. The first comprises internal modes of the intercalate molecules (e.g., Br_2 stretching modes in bromine-graphite compounds), while the second type exists only in the intercalation compound and comprises out-of-plane or in-plane vibrational modes of intercalate atoms or molecules. Out-of-plane modes are generally not well described as pure intercalate modes, since both carbon and intercalate atoms tend to have appreciable displacement amplitudes, as shown in previous studies of $[100]T_1$ and $[001]L$ phonon dispersion.^{1,2} In-plane intercalate modes, on the other hand, should be very nearly pure intercalate motions because of the great resistance of the strongly bound graphitic sheets to in-layer carbon displacements. In this article, we report the results of neutron-scattering experiments on in-layer intercalate motions in alkali-metal graphite intercalation compounds (AGIC's).

An aspect which is emphasized in the present investigation concerns the nature of the disordered phases of AGIC's, i.e., whether it is meaningful in a dynamic sense to think of the order-disorder phase transformations which occur in these materials as intercalate melting transitions, as suggested in a static sense by x-ray-diffraction experiments.³⁻⁵ In the case of stage-2 K, Rb, and Cs compounds, agreement now seems to be converging on a picture⁶ of small regions of local $\sqrt{7} \times \sqrt{7}$ registry separated by ordered domain walls in the low-temperature phase below T_0 . In the disordered phase above T_0 , the most probable picture is one in which some tendency for local $\sqrt{7} \times \sqrt{7}$ registry is maintained, but the domain

walls become diffuse, disordered, and mobile, and the intercalate layers become essentially liquidlike. On the other hand, electron-diffraction experiments^{7,8} have suggested a more complex mixed-phase behavior involving wholly or partially solidlike phase components.

A second motivation for our experiments is that the in-plane intercalate-mode spectra contain rather direct information on intercalate-intercalate and intercalate-graphite forces. Our point of view is that it is highly desirable to elucidate the physical nature of these interactions, how they depend on stage and intercalate species, and how they may come into play during staging or other rearrangements of the intercalate.

Previous studies on GIC's have focused on features of the lattice dynamics which are rather different from the present investigations of intercalate modes. (See the recent comprehensive review by Dresselhaus and Dresselhaus.⁹) High-frequency graphitic modes whose positions are slightly perturbed by the presence of the intercalate have received the most attention in Raman scattering experiments, while phonon dispersion of $[001]L$ modes has been the commonest subject of neutron experiments. In both cases, c axis and basal-plane zone-folding effects, respectively, due to staging and intercalate ordering, have important effects on the phonons. Several theoretical investigations of the lattice dynamics of GIC's have been carried out, including those of Leung *et al.*,¹⁰ Horie *et al.*,¹¹ Gupta *et al.*,¹² and Al-Jishi and Dresselhaus.¹³

II. EXPERIMENT

For the measurement of intercalate modes by neutron scattering, large sample size is highly desirable, since the scattered intensities involved are typically an order of

magnitude lower than those for [001]L phonon dispersion measurements. On the other hand, the requirement of small mosaic spread about the c axis is not nearly as stringent as for measuring, e.g., the dispersion of layer-bending (T_L) modes.¹ These considerations dictated the use of pyrolytic graphite (PG) starting material with a mosaic spread η of 5°–10° FWHM (full width at half maximum), rather than smaller highly oriented pyrolytic graphite (HOPG) specimens with $\eta < 1^\circ$. Intercalation by the usual two-zone method¹⁴ typically required several days for each of our rather large ($\approx 10 \text{ cm}^3$) samples, which had mosaic spreads between 7° and 15°.

The principle of our neutron-scattering method is to regard a PG-based GIC sample as a two-dimensional (2D) polycrystal, and to measure the in-plane phonon density of states for intercalate modes by techniques similar to those^{15,16} which have been employed for many years to determine phonon–density-of-states (PDOS) functions on 3D polycrystalline samples. Using a triple-axis spectrometer, we measured the scattering law $S(Q, \nu)$ for about five values of Q in the range 3.5–4.5 \AA^{-1} , with Q in the basal plane, and averaged the scans. A higher rate of data collection could probably be obtained on a time-of-flight spectrometer at the expense of a more complicated data analysis. The chosen Q values are much larger than the in-plane zone boundaries of ordered intercalate phases [e.g., 0.74 \AA^{-1} for a (2×2) triangular superstructure], or than $2\pi/d_{\text{NN}}$ for disordered phases, where d_{NN} is a nearest-neighbor in-plane distance. Thus, a uniform sampling over all intercalate modes with both phonon wave vectors q and atomic displacements e in the basal plane is obtained, giving the phonon density of states $g(\nu)$ via the incoherent approximation¹⁷

$$S(Q, \nu) = \frac{KQ^2\sigma}{m\nu} [n(\nu) + 1] e^{-2W} g(\nu) + M(Q, \nu). \quad (1)$$

Here, $n(\nu)$ is the Bose-Einstein factor, m and σ the mass and cross section of an intercalate atom, K a constant, and e^{-2W} is the Debye-Waller factor. The term $M(Q, \nu)$ arises from multiphonon scattering, and typically represents 20% of the intensity at room temperature and a few percent at low temperatures. Even if no correction were applied for multiphonon scattering, the $g(\nu)$ derived from a measurement would not be grossly in error, because $M(Q, \nu)$ tends to be a featureless function of ν which is not easily distinguished from a uniform background, and a background subtraction is performed before applying Eq. (1). Nonetheless, we have corrected our data for two-phonon scattering by means of the following procedure. First, the shape of the two-phonon scattering was calculated by folding the first term on the right-hand side of Eq. (1) with itself, assuming a $g(\nu)$ estimated by initially neglecting multiphonon scattering. Note that Eq. (1) applies for both neutron energy loss and gain if we take ν to be positive for the former and negative for the latter; it is the total function (positive and negative ν) which is folded with itself. Second, we recognize that to a good approximation, the ratio of the two-phonon to the one-phonon scattering is just the Debye-Waller exponent¹⁸ $W_{\parallel} = Q^2 \langle u_{\parallel}^2 \rangle / 4$, where

$$\langle u_{\parallel}^2 \rangle = \frac{\hbar}{m} \int_0^{\nu_m} g(\nu) \coth(h\nu/2kT) \nu^{-1} d\nu \quad (2)$$

is the in-plane mean-square displacement due to thermal vibrations. Thus an iterative procedure is defined in which an improved estimate of $g(\nu)$ is obtained by calculating it via two-phonon corrections which are derived from the previous estimate of $g(\nu)$. The values of $\langle u_{\parallel}^2 \rangle$ and W_{\parallel} obtained as by-products are in themselves useful data, and will be discussed in Sec. III.

In our method of in-plane scattering we implicitly tend to regard the intercalate layers as 2D solids, in that we do not look at modes with wave vectors q with out-of-plane components. If there were significant interlayer correlations in the motions of the alkali-metal atoms, these would show up as dispersion of the modes with q_z , an effect which we do not address in the present work. Dispersion with q_z may be significant for stage-1 compounds, but is probably very small for stage-2 and higher stages.

The response of the graphitic planes in the scattering geometry employed (Q parallel to the layers) is extremely weak because of the very strong in-layer bonding of the C atoms. Also, we chose values of Q to avoid the only regions of reciprocal space where scattering from low-energy in-plane graphitic modes can occur, i.e., the neighborhood of graphitic Bragg rings. The dispersion curves of graphite¹⁹ shows that no such modes exist below 6 THz unless one is within 0.12 \AA^{-1} of a graphitic Bragg ring, whereas our distance of closest approach is 0.74 \AA^{-1} . The negligible response of the graphitic planes was verified experimentally by scans on pure pyrolytic graphite at the same Q values employed for the AGIC samples.

Some further discussion of our method for measuring intercalate modes is given in a previous paper²⁰ on phonons in RbC_8 , while some of the data reported here have been described elsewhere²¹ in preliminary form.

The neutron-scattering measurements were carried out on a triple-axis spectrometer at the High Flux Isotope Reactor at Oak Ridge National Laboratory. The (002) planes of graphite were employed as monochromator and analyzer, with the scattered-neutron energy fixed at 3.3 THz and pyrolytic graphite filters in the scattered beam to remove higher diffraction orders. Typical energy-resolution widths were $\Delta E = 0.3$ and 1.0 THz at phonon energies of 1.0 and 3.0 THz, respectively.

III. RESULTS AND DISCUSSION

A. Dependence of $g(\nu)$ on alkali-metal species and stage

The phonon densities of states for the stage-1 compounds CsC_8 , RbC_8 , and KC_8 at room temperature, and that of CsC_8 at 10 K, are shown in Fig. 1. The RbC_8 data have been reported previously.²⁰ Each spectrum consists of two peaks of approximately the same area, suggestive of what one would anticipate from 2D solids comprising independent intercalate layers. Our previous study²⁰ showed that such a decoupled-layer picture is inappropriate for a stage-1 compound, but the identification of the lower- and higher-frequency peaks in $g(\nu)$ with transverse and longitudinal in-plane intercalate modes would remain

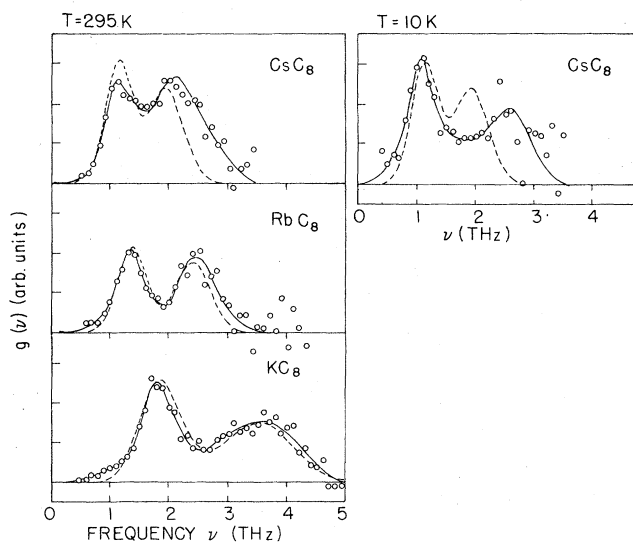


FIG. 1. In-plane phonon densities of states $g(\nu)$ for intercalate modes in stage-1 compounds, as derived from neutron-scattering experiments. Dashed curves are calculated from the Coulombic force model described in the text. The solid curves on this figure, and all the curves on subsequent figures, are merely guides to the eye, unless otherwise noted.

valid in any reasonable model, even when long-range 3D interactions are included. Compared with RbC_8 , the frequencies in CsC_8 at room temperature are somewhat higher, and those in KC_8 somewhat lower, than one would expect solely on the basis of the metal-atom mass change; i.e., $\langle \nu \rangle_{\text{K}} / \langle \nu \rangle_{\text{Rb}} = 1.43$ and $\langle \nu \rangle_{\text{Cs}} / \langle \nu \rangle_{\text{Rb}} = 0.87$ from experiment, whereas $(m_{\text{Rb}}/m_{\text{K}})^{1/2} = 1.478$ and $(m_{\text{Rb}}/m_{\text{Cs}})^{1/2} = 0.802$. The room-temperature spectrum for CsC_8 is less distinctly separated into two peaks than the spectra of the other two compounds, indicating a greater degree of anharmonicity and/or structural disorder in the Cs case. In the 10-K spectrum of CsC_8 , a well-resolved two-peak structure is observed, and the upper peak rises in frequency from 2.2 to 2.6 THz, a surprisingly large change which favors anharmonicity as the cause of broadening at room temperature. The amplitude of the upper peak relative to the lower is smaller at low temperature, not only for CsC_8 but also for all the other AGIC's we have examined, a possible indication that our correction procedure for multiphonon scattering is not completely adequate, or that multiple-scattering effects need to be considered.

The shapes of these in-plane phonon densities of states contain significant information about the interaction be-

tween intercalate metal (M) atoms and between M atoms and graphitic planes (M -C interaction). Our previous analysis²⁰ of $g(\nu)$ for RbC_8 showed that a 2D Born-von Kármán model with nearest-neighbor M - M forces plus a short-range M -C coupling (two adjustable parameters) fits the spectrum poorly. A much better fit was provided by a model in which the M -C coupling is retained, but in which the M - M interactions are long-range Coulomb forces between M^+ ions. This model has only one adjustable parameter, ν_0 , which arises from the M -C interaction and is simply the in-plane frequency of an M atom in the absence of direct M - M forces; i.e., $m\nu_0^2$ is the curvature of the egg-carton-like potential due to the bounding graphitic layers felt by an average M atom. In the case of stage-1 registered AGIC's, the appropriate curvature is that at the bottoms of the depressions at graphitic hexagon centers, while for stage- $(n \geq 2)$ incommensurate phases static displacements away from hexagon centers may be present and a curvature averaged over actual M positions would apply. The dashed curves in Fig. 1 represent calculations of $g(\nu)$ for stage-1 compounds based on this Coulombic force model. The best fits to the observed spectra are obtained by adjusting ν_0 to values slightly below the frequency of the lower-energy peak. The fitted values are listed in Table I. In the absence of M -C coupling, this model predicts that the upper peak occurs very close to the ion-plasma frequency $\nu_p = e/(\pi m V)^{1/2}$, where V is the volume per M^+ ion, shifting to $(\nu_0^2 + \nu_p^2)^{1/2}$ when the M -C interaction is taken into account. Table I shows that the observed upper-peak frequencies are indeed very close to $(\nu_0^2 + \nu_p^2)^{1/2}$ for RbC_8 and KC_8 . For CsC_8 the observed frequency is somewhat higher than the predicted one, possibly because of direct short-range overlap forces between the large Cs ions. The extent of the discrepancy is also illustrated in the comparison of the 10-K experimental spectrum for CsC_8 with the calculated spectrum in Fig. 1. All the calculated spectra in Fig. 3 have been subjected to a Gaussian-broadening process, in which the full width of the Gaussian increases linearly with frequency, from 0.4 THz at a frequency of 1.0 THz to 1.2 THz at a frequency of 3.5 THz. This procedure allows for the effects of experimental resolution, anharmonicity and extra dispersion not accounted for by the Coulombic model. At frequencies below 2 THz, the dominant broadening is that of resolution, but at higher frequencies the other factors must also have some effect. The presence of extra dispersion would, of course, indicate that the Coulombic model is not completely adequate. Nonetheless, the degree of agreement with the model, particularly for KC_8 and RbC_8 , is surprisingly good.

A factor which is neglected in the picture implied by the Coulombic force model is the screening contribution

TABLE I. Values of ν_0 and ion-plasma frequency ν_p , in THz. The observed positions ν_{obs} of the upper peaks in the intercalate-mode spectra are close to $\nu_c = (\nu_0^2 + \nu_p^2)^{1/2}$.

	T (K)	ν_0	ν_p	ν_c	ν_{obs}
KC_8	296	1.60	3.20	3.58	3.65
RbC_8	296	1.20	2.10	2.42	2.50
CsC_8	10	1.00	1.64	1.92	2.6

due to readjustment of the conduction-electron distribution in response to the motion of the ion cores. In most metals this contribution has a dominant effect on the phonon frequencies and, indeed, is considered the only non-trivial part of lattice-dynamical calculations. In alkali metals²² the maximum phonon frequency ν_m is renormalized downward from ν_p to about $0.5\nu_p$ by conduction-electron screening, and the effect is even larger for polyvalent metals ($\nu_m/\nu_p \approx 0.2$ for Pb). Thus it is rather surprising that screening can be neglected for in-plane M modes in stage-1 AGIC's. However, it is not correct to conclude that this implies complete charge transfer of the valence electrons of the alkali-metal atoms to the graphitic layers. All that is really implied is that the conduction-electron charge distribution, whether situated on graphitic or intercalate layers, is quite rigid, and does not readjust significantly in response to ionic motions. DiVincenzo and Mele²³ have recently predicted that the screening length due to carriers on a graphitic layer is rather large, ~ 4 Å. Thus there is some theoretical basis for believing that conduction electrons on graphitic layers would not be able to screen large- q phonons.

The dependence of $g(\nu)$ on stage number at room temperature for the Rb-graphite system is shown in Fig. 2. As before, the stage-1 spectrum is from Ref. 20. The spectra are again fairly similar in shape, except that the two constituent peaks are unresolved for stage-2 RbC₂₄ and stage-3 RbC₃₆. As we have noted in the case of CsC₈, this could arise from two factors, anharmonicity and dis-

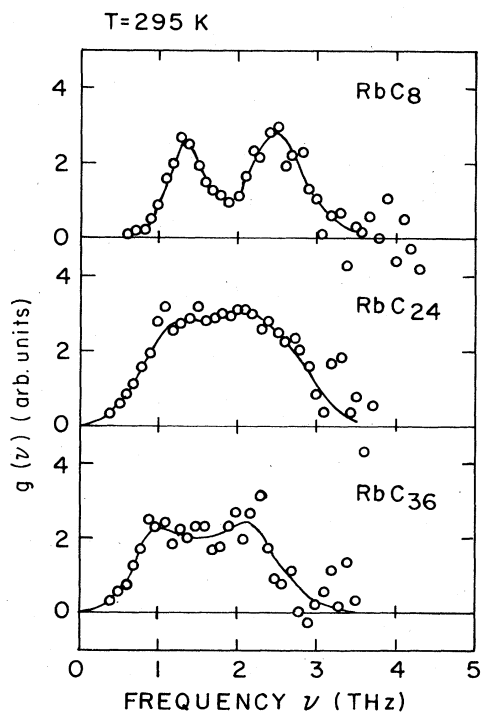


FIG. 2. Intercalate-mode phonon densities of states $g(\nu)$ for Rb-graphite compounds. The stage-1 compound is RbC₈, while RbC₂₄ and RbC₃₆ are, respectively, the stage-2 and -3 compounds.

order. RbC₂₄ undergoes an order-disorder phase transition at 162 K and hence has substantial disorder in the Rb substructure at room temperature. One would expect a similar amount of disorder to be present in RbC₃₆. It is difficult to estimate whether anharmonicity or disorder is more important in producing broadening of the stage-2 and -3 spectra, although probably both are significant. There is a noticeable drop in the average frequency as one goes from RbC₈ to RbC₂₄, and perhaps again from RbC₂₄ to RbC₃₆. The drop from stage 1 to 2 must arise primarily from a decrease in the average Rb-Rb in-layer force constants due to the lower intercalate layer density in RbC₂₄. The further apparent drop upon going to stage 3 is, we believe, not significant, since a more quantitative comparison with stage-2 spectra shows no real differences, as we discuss in the following paragraph.

The in-plane Debye-Waller exponents W_{\parallel} and the implied mean-square displacements $\langle u_{\parallel}^2 \rangle$ due to thermal vibrations derived from the analysis of our experimental $g(\nu)$ functions are shown in Fig. 3. The softening of the $g(\nu)$ spectra upon going from Cs to Rb to K within the stage-1 compounds is manifested in the increasing values of the points at 300 K, while the yet higher points for KC₂₄ and RbC₃₆ imply spectra that are even softer for those materials. All the stage-2 points and the stage-3 RbC₃₆ point lie on a single curve, suggesting M - M interactions that are independent of stage and alkali-metal species for stages $n \geq 2$. A possible reason for this may lie in the lower layer densities of high-stage compounds in comparison to stage-1 materials, i.e., short-range forces due to direct "contact" between nearest-neighbor M atoms produce a dependence on M for stage 1 but not for higher stages. Recent x-ray-diffraction measurements on RbC₂₄ by Ohshima *et al.*²⁴ imply values of W_{\parallel} and $\langle u_{\parallel}^2 \rangle$ that are substantially larger than our values. They observe $B_{\parallel} = 8.32 \pm 0.09$ Å² at 297 K, compared with $B_{\parallel} = 3.94$ Å² derived from our data. This is evidence that there are static displacements of K atoms away from the registered positions defined by graphite hexagon centers, which provide an extra contribution to the x-ray Debye-Waller factor. We would expect such displacements on the basis of our interpretation of the shapes of the $g(\nu)$ spectra. The M - C interaction, which tends to force the K atoms into registry and has a strength proportional to ν_0^2 , is weaker

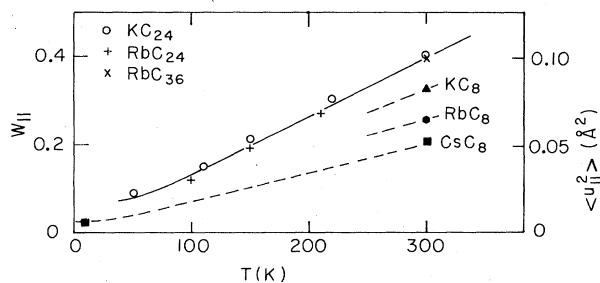


FIG. 3. In-plane components of the Debye-Waller exponent W_{\parallel} and mean-square vibrational amplitude $\langle u_{\parallel}^2 \rangle$ for the intercalate atoms, derived from the measured intercalate-mode spectra. $W_{\parallel} = W_{\parallel}(Q)$, where $Q = 4$ Å⁻¹.

than the M - M interaction, which has a strength proportional to v_p^2 . The static displacements are not expected for stage-1 registered phases, but should be present for the incommensurate structures which form for higher stages. Thus, even though the standard picture⁶ of locally registered $\sqrt{7} \times \sqrt{7}$ domains separated by discommensurations may be qualitatively correct for stage- $(n \geq 2)$ compounds, most of the atoms should be considerably displaced from registry, especially those near the discommensurations.

Other work relevant to the present investigations on intercalate modes in AGIC's are (i) measurements of specific heats,²⁵⁻²⁷ and (ii) lattice-dynamical calculations by Al-Jishi and Dresselhaus¹³ and Kimura *et al.*²⁸ The specific heats of stage-(1-4) AGIC's are enhanced at low temperatures by the intercalate modes; the enhancement can be fitted by Einstein oscillators whose frequencies generally correspond to the lower of the two peaks in $g(\nu)$ observed by us. The upper peak produces contributions to the specific heat at higher temperatures, where the enhancement is difficult to distinguish from the larger contribution from graphitic modes. Of course, not only in-plane modes but also out-of-plane intercalate modes contribute to the specific-heat enhancement. Our previous neutron studies¹ of out-of-plane $[100]T_1$ modes showed that, besides being strongly coupled to graphitic modes, the lowest-energy modes of stage-2 compounds were modified by a weakening of the interlayer shear resistance to produce a phonon dispersion nearly of the form $\nu \sim q^2$. It is thus not certain that the lattice contribution to the specific heat varies as T^3 over the range spanned by the heat-capacity measurements. We conclude that whereas there is already a good qualitative correspondence among specific-heat experiments, our neutron experiments, and existing lattice-dynamical calculations, further refinement of the calculations to fit our data in detail might allow new information to be extracted from the specific-heat data.

B. Temperature dependence for KC_{24} , RbC_{24} , and RbC_8 : Relation to order-disorder transformations

One of the most interesting and heavily studied structural phenomena exhibited by alkali-metal graphite intercalation compounds is the occurrence of order-disorder phase transformations in the intercalate substructure.³⁻⁵ In-plane x-ray-diffraction patterns show a solid-like pattern, i.e., Bragg peaks, below some transition temperature T_0 , and only liquidlike diffuse scattering above T_0 . The initial interpretations of such observations were naturally in terms of melting transitions of the intercalant substructure, of a quasi-two-dimensional character for higher stages. More quantitative reexaminations of the x-ray data led to some refinement of this idea, and the predominant interpretation^{6,29} of the x-ray data on stages $n \geq 2$ at the present time is that at low temperatures there is local $\sqrt{7} \times \sqrt{7}$ registry within microdomains ~ 40 Å in size, with the microdomains separated by a honeycomb structure of discommensurations or domain walls. The most likely picture of the disordered phase assuming this

model would involve disordering of the domain walls and persistence of local $\sqrt{7} \times \sqrt{7}$ regions which are now irregular in shape and size and somewhat less well registered than in the low-temperature phase. One can still regard the transitions as melting of the intercalant layers, but with a greater role played by the influence of the bounding graphite layers. We should also mention at this point the electron-diffraction experiments^{7,8} which are, in general, inconsistent with the x-ray experiments, indicating for stage-2 compounds a complicated mixture of solid phases above T_0 .

The question which we pose in the present neutron-scattering experiments is whether the dynamical (diffusional and vibrational) properties of the intercalates in the disordered phases of AGIC's are like those conventionally associated with liquids. In other words, are the changes in the spectra of in-plane intercalate motions like what one would normally expect in a melting transition? In simple monatomic liquids like those of alkali metals, the onset of melting produces a drastic change in the low-energy portions of the spectra. Scattering that is exactly elastic disappears because the atoms no longer have time-averaged equilibrium positions, and is replaced by quasielastic scattering which has a substantial energy width. At large Q the width becomes comparable to the energies of phonons in the solid and is produced by diffusive motions which are occurring on the same timescale as vibrational motions, i.e., the qualitative distinction between the two types of motions has ceased to exist.

In Fig. 4 we show the temperature dependence of

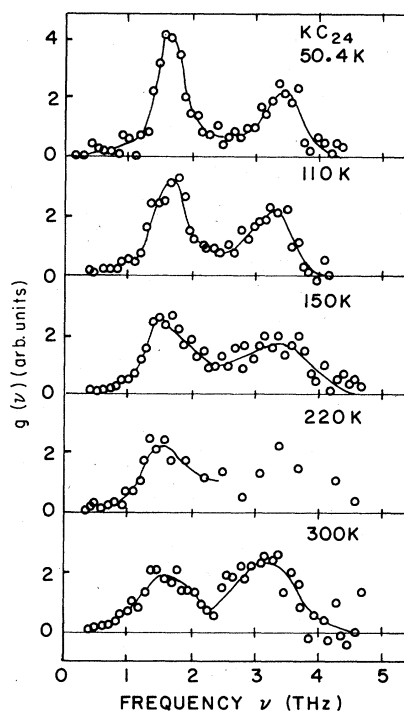


FIG. 4. Temperature dependence of intercalate-mode phonon density of states $g(\nu)$ for stage-2 potassium-graphite. An order-disorder phase transformation of the intercalate layers takes place at 123 K.

intercalate-mode phonon densities of states derived from our measurements on KC_{24} through the order-disorder transformation at $T_0=123$ K. Although the spectra broaden somewhat at higher temperatures, nothing takes place at T_0 that renders spectra above T_0 dramatically different from those below T_0 . At all temperatures the spectra are qualitatively similar, consisting of two main peaks corresponding to transverse and longitudinal in-plane intercalate modes. Similar results were obtained for RbC_{24} ($T_0=162$ K), as shown in Fig. 5. Again, the spectra above and below T_0 are qualitatively similar, but the upper peak decreases in frequency with increasing temperature more markedly than in KC_{24} , declining from 2.6 THz at 150 K to ~ 2.1 THz at 210 K, a surprisingly large effect if it is solely due to anharmonicity. We note that recent NMR experiments³⁰ on CsC_{24} also indicate surprisingly large anharmonicity of intercalate modes, as evidenced by their effect on the quadrupolar spin-lattice relaxation rate.

It may be argued that the consistently solidlike appearance of the spectra shown in Figs. 4 and 5 arises partly because of the reduction to phonon densities of states, which are forced to go to zero at zero frequency, consequently always generating a transverse-acoustic-like peak at low energies. Thus it is of interest to compare the scattering law $S(Q,\nu)$, which was directly observed in the neutron experiment, for RbC_{24} in the disordered state with that of a real 3D liquid. In Fig. 6 such a comparison is made at $Q=4 \text{ \AA}^{-1}$ for T somewhat above T_0 for RbC_{24} and somewhat above the melting point for liquid Rb.³¹ The

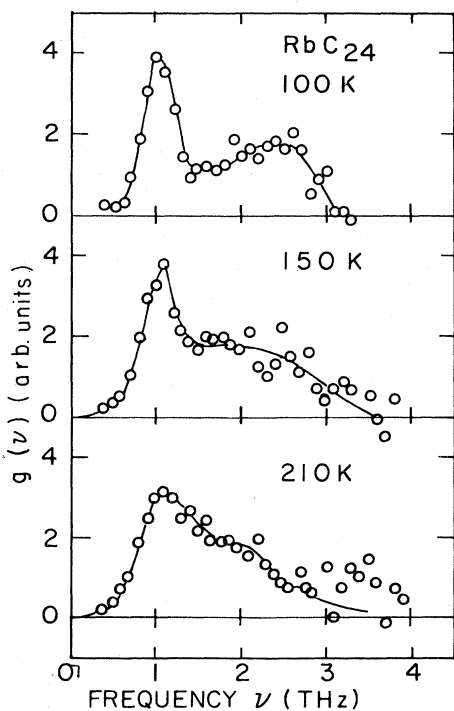


FIG. 5. Temperature dependence of intercalate-mode phonon density of states $g(\nu)$ for stage-2 rubidium-graphite. An order-disorder phase transformation of the intercalate layers takes place at 162 K.

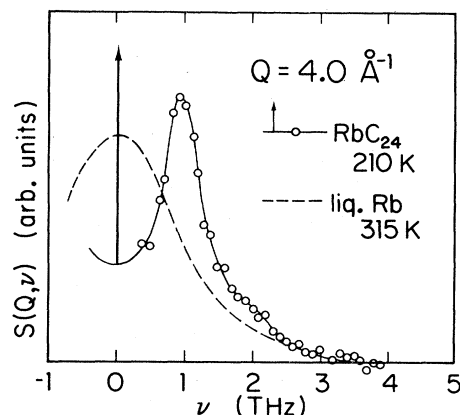


FIG. 6. Comparison of the scattering law of liquid Rb (Ref. 31) with that of the disordered intercalate in RbC_{24} . The arrow represents (Ref. 32) a sharp peak at $\nu=0$.

spectra are qualitatively different. At this relatively large wave vector, $S(Q,\nu)$ for liquid Rb consists of a single broad peak centered around zero energy. In contrast, the RbC_{24} spectrum has a pronounced peak at 1.0 THz and a very narrow, high peak at zero energy. The latter observation comes not from the present experiment, but from a recent quasielastic neutron-scattering study.³² The peak at $\nu=0$ in the RbC_{24} spectrum of Fig. 6, although very sharp, does have a finite energy width, estimated to be ~ 0.01 THz by extrapolation of the quasielastic data to the larger wave vectors and lower temperatures involved in the present experiment. This is indicative of Rb diffusion occurring on a time scale much slower than that of lattice vibrations. In liquid Rb the observation of a single broad peak means that for the short wavelengths implied by $Q=4 \text{ \AA}^{-1}$, there is no qualitative distinction between diffusional and vibrational motion, both occurring on the same timescale. The dynamical characteristics of the 2D disordered intercalate in RbC_{24} are thus rather different from those of a 3D liquid metal.

The order-disorder transformation in RbC_{24} does have a demonstrable influence on the vibrational spectrum, as shown in Fig. 7, but the effect is a relatively subtle one. The width of the 1.0-THz peak in $S(Q,\nu)$, plotted against T , increases more rapidly immediately above T_0 . The

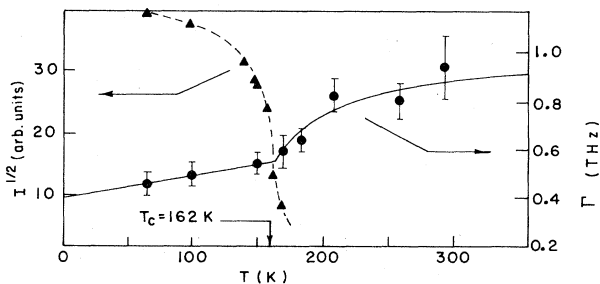


FIG. 7. Temperature dependence of the order parameter, as measured through the square root of the intensity I of an intercalate Bragg peak, and the temperature dependence of the energy width of the 1-THz inelastic peak in RbC_{24} .

temperature dependence of the long-range order below T_0 , as measured by the square root of the intensity of the intercalate Bragg ring at $Q=1.78 \text{ \AA}^{-1}$, is also shown in Fig. 7. No hysteresis of the Bragg scattering within the precision of temperature control, about 0.2 K, was observed, in agreement with results of Hastings *et al.*³³ on KC_{24} , but at odds with other data³⁴ reporting several degrees hysteresis in RbC_{24} . Our data can be fitted with a transition temperature $T_c=162.2\pm 3.0 \text{ K}$, and a critical exponent for the long-range order $\beta=0.185\pm 0.040$, very close to the value 0.18 ± 0.01 obtained by x-ray diffraction for KC_{24} .³⁵ We believe that this transition is second order, or has a very small first-order discontinuity. Theoretical arguments³⁶ that the transition should be a smeared first-order one, because of stacking-fault disorder below T_c , may be, in principle, correct, but we believe that the characteristics of the transition are dominated by intralayer Rb-Rb interactions, the much weaker interlayer interactions serving mainly to establish 3D order below T_c . The value of β is somewhat larger than the $\beta\approx 0.12$ expected for a 2D system, but much smaller than the $\beta\approx 0.33$ expected for a 3D system. The situation is reminiscent of quasi-2D antiferromagnets, which display long-range 3D order below T_c , but have critical exponents characteristic of 2D systems.

Stage-1 AGIC's disorder at considerably higher temperatures than do stage-2 compounds, e.g., 745 K for RbC_8 , compared with 162 K for RbC_{24} . It may, in fact, be argued that the transformations are qualitatively dissimilar, since one takes place in thermodynamic equilibrium at high temperature and is associated with a change in the composition of the compound, while the other is a subtle low-temperature rearrangement of the intercalate in a metastable compound which has been quenched rapidly after formation at high temperature. Furthermore, the stage-1 transformation temperature is dependent on external vapor pressure,³⁷ unlike the case for stage 2. With respect to x-ray-diffraction characteristics, however, the transformations are similar.

Elastic- and inelastic-neutron-scattering measurements were carried out on RbC_8 to investigate structural and vibrational changes associated with the order-disorder transformation in a stage-1 AGIC. As in the previous neutron-diffraction work of Ellenson *et al.*,³⁸ we observed a stacking-order change from $\alpha\beta\gamma\delta$ to $\alpha\beta\alpha\beta$ at 720 K, followed by the order-disorder transformation at 745 K. It should be noted that the latter temperature applies only to an external vapor pressure corresponding to the vapor pressure above liquid Rb at 745 K. It is well known that the stoichiometry changes from RbC_8 to roughly RbC_{10} as the disordering occurs, accompanied by a color change from copperish to purple. We observed little or no hysteresis at either transformation, in contrast to the large hysteresis³ reported for CsC_8 in the presence of excess Cs metal. We found that the order-disorder transformation was rather sluggish, requiring up to an hour to reach completion—not unusual considering the large size of our sample and the fact that 20% of the intercalate must be expelled and reabsorbed as one cycles through the transition—but the transition temperatures on heating and cooling were identical to within the measurement pre-

cision of two degrees.

Inelastic scattering measurements of the spectra of in-plane motions in RbC_8 were carried out as a function of temperature from 12 to 750 K. At temperatures below about 500 K the spectra are similar to the room-temperature spectrum for RbC_8 shown in Fig. 2, except that the frequencies of the two major peaks show an unusually large temperature dependence, presumably due to the highly anharmonic character of the egg-carton-like alkali-metal-graphite potential. The positions of the peaks versus temperature are given in Fig. 8. Above 500 K the upper peak in the spectrum becomes difficult to distinguish, and reduction to a phonon density of states is questionable because of the dominance of multiphonon scattering. Therefore, in order to compare the scattering in the ordered and disordered states, we restrict ourselves to a direct comparison of $S(Q, \nu)$ somewhat below (700 K), immediately below (723 K), and immediately above (750 K) the phase transformation, as shown in Fig. 9. Unlike the case for stage-2 compounds, we now observe a discontinuous change through the phase transformation. The minimum at 0.65 THz tends to fill in and the maximum at 1.1 THz becomes less well defined. Such behavior is vaguely reminiscent of what one would see in the melting of a 3D liquid, where the minimum would totally disappear and the vibrational spectrum would become merged with a broad diffusional peak at $\nu=0$. However, it is certainly qualitatively more like the behavior of the stage-2 compounds as described above, and one anticipates that there is a peak at $\nu=0$ with a narrow diffusional width which we have not resolved in our measurements on RbC_8 (the strong peak at $\nu=0$ in the scans of Fig. 9 is mainly due to scattering from the graphite host).

If we accept a basically liquidlike picture for the disordered phases of AGIC's, the principal result of our data that we must explain is that, in contrast to real 3D liquids, diffusion occurs on a much slower timescale than do vibrations. Two possibilities which may give rise to this qualitatively different behavior are (i) the effect of the

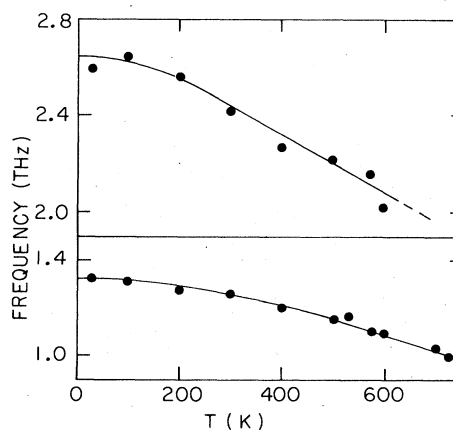


FIG. 8. Temperature dependence of the frequencies of the two peaks in the intercalate mode spectrum of stage-1 Rb-graphite.

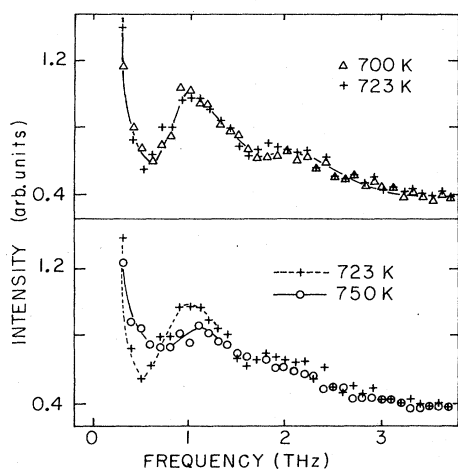


FIG. 9. Scattering from stage-1 Rb-graphite in the vicinity of the order-disorder transformation at 745 K.

egg-carton-like potential due to the graphitic layers, and (ii) restriction of the alkali-metal M atoms to planar motion. With regard to (i), the M -graphite interaction must directly hinder diffusion to some extent, tending to constrain the M atoms to lie laterally closer to the centers of graphitic hexagons, even in the disordered phase. The position of the lower-energy peak in $g(\nu)$ or $S(Q, \nu)$ is determined by the M -graphite potential, as discussed in the preceding subsection, and the fact that the peak in all cases persists in the disordered phase implies that the M atoms still lie close to hexagon centers above T_0 . With regard to (ii), it may be that the restriction to planar geometry greatly inhibits diffusion, making the motions involved more collective in character and necessarily slower than vibrations. Computer simulations of $S(Q, \nu)$ for a 2D liquid would be very useful in the interpretation of our data, but to our knowledge no such calculations exist.

From another point of view, (i) and (ii) are but different aspects of the same mechanism, which one might regard simply as steric hindrance. One would expect that a tortuously connected and bumpy 3D channel structure within a rigid host would provide a hindering of diffusive motions, much as in the present case of disordered AGIC's, and that dimensionality as such is involved only indirectly. Metal hydrides and ionic conductors are physical realizations of such a situation, in which diffusion of the mobile species can occur on time scales intermediate between those of ordinary solid-state and liquid-state diffusion. Another even more closely related situation occurs in the order-disorder transitions of atoms or molecules on surfaces. For rare gases adsorbed on graphite these transitions are commonly regarded as 2D melting.

The transitions in AGIC's are very similar in character, except that the corrugation potential due to the graphitic "substrate" plays a greater role. It is not inconsistent to regard the disordered phases of AGIC's both as highly viscous liquids and aggregates of solidlike locally registered microcrystals separated by a disordered and mobile network of discommensurations or domain walls. The liquid picture becomes more appropriate for T far above T_0 , while the disordered discommensuration picture has greatest validity just above T_0 . The interrelationship between the discommensuration domain structure and the dynamical behavior of the alkali-metal intercalate layers in stage-2 compounds will be discussed in more detail in a forthcoming paper.³⁹

IV. SUMMARY AND PERSPECTIVE

The in-plane spectra of intercalate motions in AGIC's show dependences on alkali-metal species and stage number that mainly arise from differences in intercalate atomic masses and layer densities. The interactions between intercalate atoms are largely ionic in character, conduction-electron screening of the ion motions having surprisingly little influence. While the intercalate-intercalate interactions are generally stronger than the intercalate-graphite interactions, the latter are not small, involving forces about one-quarter the size of the former. Disorder in the intercalate layers and anharmonicity sometimes have a strong broadening effect on the spectra, especially for lower layer densities (i.e., stages 2 and 3) and for higher temperatures.

Our measurements of the temperature dependence of the spectra of RbC_{24} , KC_{24} , and RbC_8 indicate only subtle changes due to their order-disorder transformations. Steric hindrance due to the graphitic host makes diffusion occur in the disordered intercalate phases on a time scale much slower than vibrations, unlike simple 3D liquids, where the two occur on the same time scale. These results may have a wider relevance, since apparently similar order-disorder and 2D melting phenomena also occur for monolayers of adsorbed atoms or molecules on surfaces.

ACKNOWLEDGMENTS

We especially wish to thank R. M. Nicklow for making available to us the use of neutron-scattering facilities at the High Flux Isotope Reactor of Oak Ridge National Laboratory, and also for helpful advice and discussions. Ames Laboratory is operated for the United States Department of Energy (U.S. DOE) by Iowa State University under Contract No. W-7405-Eng-82. Research at the University of Illinois was supported by the U.S. DOE under Contract No. DE-AC02-76ER01198. All support for this work was managed by the Director for Energy Research, Office of Basic Energy Sciences, U.S. DOE.

¹H. Zabel, W. A. Kamitakahara, and R. M. Nicklow, Phys. Rev. B **26**, 5919 (1982).

²H. Zabel and A. Magerl, Phys. Rev. B **25**, 2461 (1982).

³R. Clarke, N. Caswell, and S. A. Solin, Phys. Rev. Lett. **42**, 61 (1979).

⁴R. Clarke, N. Caswell, S. A. Solin, and P. M. Horn, Phys. Rev. Lett. **43**, 2018 (1979).

⁵H. Zabel, Y. M. Jan, and S. C. Moss, Physica **99B**, 453 (1980).

⁶R. Clarke, J. N. Gray, H. Homma, and M. J. Winokur, Phys. Rev. Lett. **47**, 1407 (1981).

- ⁷N. Kambe, G. Dresselhaus, and M. S. Dresselhaus, *Phys. Rev. B* **21**, 349 (1980).
- ⁸A. N. Berker, N. Kambe, G. Dresselhaus, and M. S. Dresselhaus, *Phys. Rev. Lett.* **45**, 1452 (1980).
- ⁹M. S. Dresselhaus and G. Dresselhaus, *Adv. Phys.* **30**, 139 (1981).
- ¹⁰S. Y. Leung, G. Dresselhaus, and M. S. Dresselhaus, *Phys. Rev. B* **24**, 6083 (1981).
- ¹¹C. Horie, M. Maeda, and Y. Kuramoto, *Physica* **99B**, 430 (1980).
- ¹²H. C. Gupta, R. S. Narayanan, N. Rani, and V. V. Tripathi, *Synth. Met.* **7**, 347 (1983).
- ¹³R. Al-Jishi and G. Dresselhaus, *Phys. Rev. B* **26**, 4523 (1982).
- ¹⁴A. Hérold, *Bull. Soc. Chim. Fr.* **187**, 999 (1955); D. E. Nixon and G. S. Parry, *J. Phys. D* **1**, 291 (1968).
- ¹⁵M. M. Bredov, B. A. Kotov, N. M. Okuneva, V. S. Oskotskii, and A. L. Shakh-Bugadov, *Fiz. Tverd. Tela (Leningrad)* **9**, 287 (1967) [*Sov. Phys.—Solid State* **9**, 214 (1967)].
- ¹⁶B. P. Schweiss, B. Renker, E. Schneider, and W. Reichardt, in *Superconductivity in d- and f-Band Metals*, edited by D. H. Douglass (Plenum, New York, 1976), p. 189.
- ¹⁷W. Marshall and S. Lovesey, *The Theory of Thermal Neutron Scattering* (Clarendon, Oxford, 1971), discussion on p. 94 and pp. 102 and 103.
- ¹⁸*The Theory of Thermal Neutron Scattering*, Ref. 17, pp. 74 and 75.
- ¹⁹R. M. Nicklow, N. Wakabayashi, and H. G. Smith, *Phys. Rev. B* **5**, 4951 (1972).
- ²⁰W. A. Kamitakahara, N. Wada, S. A. Solin, and L. M. Seaverson, *Phys. Rev. B* **28**, 3457 (1983).
- ²¹W. A. Kamitakahara and H. Zabel, in *Intercalated Graphite*, edited by M. S. Dresselhaus, G. Dresselhaus, J. E. Fischer, and M. J. Moran (North-Holland, New York, 1983), p. 317.
- ²²D. L. Price, K. S. Singwi, and M. P. Tosi, *Phys. Rev. B* **2**, 2983 (1970).
- ²³D. DiVincenzo and E. J. Mele, *Phys. Rev. B* **29**, 1685 (1984).
- ²⁴K. Ohshima, S. C. Moss, and Roy Clarke, in *Proceedings of the International Symposium on Graphite Intercalation Compounds*, Tsukuba, Japan, 1985 [*Synth. Met.* (to be published)].
- ²⁵U. Mizutani, T. Kondow, and T. B. Massalski, *Phys. Rev. B* **17**, 3165 (1978).
- ²⁶M. Suganuma, T. Kondow, and U. Mizutani, *Phys. Rev. B* **23**, 706 (1981).
- ²⁷M. G. Alexander, D. P. Goshorn, and D. G. Onn, *Phys. Rev. B* **22**, 4535 (1980).
- ²⁸T. Kimura, R. Yamamoto, and M. Doyama, *J. Phys. F* **12**, 907 (1982).
- ²⁹M. Suzuki and H. Suematsu, *J. Phys. Soc. Jpn.* **52**, 2761 (1983).
- ³⁰F. Borsa, M. Corti, A. Rigamonti, and S. Torre, *Phys. Rev. Lett.* **53**, 2102 (1984).
- ³¹J. R. D. Copley and J. M. Rowe, *Phys. Rev. A* **9**, 1656 (1974).
- ³²H. Zabel, A. Magerl, A. J. Dianoux, and J. J. Rush, *Phys. Rev. Lett.* **50**, 2094 (1983).
- ³³J. B. Hastings, W. B. Ellenson, and J. E. Fischer, *Phys. Rev. Lett.* **42**, 1552 (1979).
- ³⁴I. Naiki and Y. Yamada, *J. Phys. Soc. Jpn.* **51**, 257 (1982).
- ³⁵H. Zabel, S. C. Moss, N. Caswell, and S. A. Solin, *Phys. Rev. Lett.* **43**, 2022 (1979).
- ³⁶P. Bak and E. Domany, *Phys. Rev. B* **23**, 1320 (1981).
- ³⁷N. Caswell, *Phys. Rev. B* **22**, 6308 (1980).
- ³⁸W. B. Ellenson, D. Semmingsen, D. Guerard, D. G. Onn, and J. E. Fischer, *Mater. Sci. Eng.* **31**, 137 (1977).
- ³⁹H. Zabel, M. Suzuki, D. A. Neumann, S. E. Hardcastle, A. Magerl, and W. A. Kamitakahara, in *Proceedings of the International Symposium on Graphite Intercalation Compounds*, Tsukuba, Japan, 1985, Ref. 24.